IEEE Access
Multidisciplinary | Rapid Review | Open Access Journal

Received 2 June 2023, accepted 11 July 2023, date of publication 19 July 2023, date of current version 25 July 2023.

Digital Object Identifier 10.1109/ACCESS.2023.3296990

RESEARCH ARTICLE

Seamless Power Management for Decentralized DC Microgrid Under Voltage Sensor Faults

DAT THANH TRAN[1], MYUNGBOK KIM[2], (Member, IEEE), AND KYEONG-HWA KIM[1], (Senior Member, IEEE)

[1]Department of Electrical and Information Engineering, Research Center for Electrical and Information Technology, Seoul National University of Science and Technology, Nowon-gu, Seoul 01811, South Korea
[2]Automotive Components and Material Research and Development Group, Korea Institute of Industrial Technology, Buk-gu, Gwangju 61012, South Korea

Corresponding author: Kyeong-Hwa Kim (k2h1@seoultech.ac.kr)

This work was supported by the Korea Institute of Industrial Technology as Development of Core Technologies of AI-Based Self-Power Generation and Charging for Next-Generation Mobility under Grant KITECH EH-23-0013.

ABSTRACT In this paper, a seamless power management scheme is proposed for a decentralized DC microgrid (DCMG) to maintain voltage stabilization in the presence of voltage sensor faults. First, a voltage observer is constructed in each power agent to monitor the voltage sensor abnormality under various uncertain conditions. During the normal operations, the power balance as well as the voltage regulation of the DCMG is achieved by using the voltage droop control method which consists of the secondary controller and primary controller. While the secondary controller is utilized to maintain the DC-link voltage (DCV) at the nominal value, the power balance is achieved by the droop control method in the primary controller. In both controllers, the estimated DCV value is employed as the only feedback signal from the DC-link to the power agent. To maintain a seamless power management even under DCV sensor faults, a fault identification algorithm is first presented to detect voltage sensor failure. After the power agent recognizes its DCV sensor fault, its operation mode is switched from the voltage control to the current control mode, in which the operating point in the droop curves is perturbed by changing the current magnitude in the power agent with the faulty DCV sensor. The perturbation of operating point in the droop curves makes the other power agents with normal DCV sensor take a control of DCV instead of the power agent with the faulty DCV sensor to guarantee voltage stabilization and prevent the system collapse. Furthermore, the proposed scheme adjusts appropriately the droop curve of the utility grid agent in the primary controller under high electricity price condition to minimize electricity costs. Simulation and experimental results under various conditions verify the effectiveness and reliability of the proposed seamless power management strategy.

INDEX TERMS DC microgrid, decentralized system, droop control, seamless power management, secondary control, voltage restoration, voltage sensor fault.

I. INTRODUCTION

In recent decades, the microgrid is extensively used as an effective method not only to ensure the electricity demand caused by industrialization and modernization trends but also to increase the scalability and flexibility of the utility grid [1], [2]. The microgrid is a small-scale power system which is commonly integrated by the utility grid, energy storage systems (ESSs), load, and renewable energy sources (RESs) such as wind or solar power sources [3], [4]. In general, the microgrid system is divided into two categories: DC microgrid (DCMG) and AC microgrid (ACMG). In comparison to the ACMG, the DCMG has received raised levels of attention from researchers because of its high system efficiency, outstanding power quality, and simple control [5], [6].

The operation of a DCMG system can be classified into the islanded mode and grid-connected mode depending on the availability of the utility grid [7]. Traditionally, in the grid-connected mode, the power balance and voltage stabilization are maintained by the utility grid agent [8]. In this mode,

The associate editor coordinating the review of this manuscript and approving it for publication was S. K. Panda.

the DCMG system should take into account the minimum electricity cost for the utility grid to reduce the operation cost in the DCMG [9], [10]. In the islanded mode, the power agents in DCMG are coordinated properly to ensure power-sharing even under several uncertain conditions such as agent power variation, the ESS state-of-charge (SOC) levels, and plug-and-play power agent [11].

Inspired by these concerns, several studies for effective control and management strategies for the DCMG have been proposed lately in the literature [12], [13], [14], [15], [16]. Depending on the communication perspective of a DCMG, these control strategies are separated into centralized control, distributed control, and decentralized control. In centralized control, the data of each power agent is collected by a central controller via digital communication links (DCLs) to manage the power in the DCMG system [12], [13]. On the other hand, distributed control does not rely on the use of a central controller. Instead, each power agent in distributed DCMG system independently determines its operation mode based on received information from neighbor power agents through DCLs [14], [15]. It is worth mentioning that both centralized and distributed controls suffer from many drawbacks related to high system costs, low flexibility, and transmission delay time caused by DCLs. To address these weaknesses, decentralized control is considered as an effective solution due to the absence of DCL in the DCMG system, which leads not only to optimizing the system price but also to enhancing the system scalability significantly [16].

Generally, in decentralized control, the droop control method is normally utilized in each power agent not only to regulate the DC-link voltage (DCV) but also to coordinate the power in the DCMG system [17], [18], [19], [20]. In the study [17], a decentralized control strategy based on $V^2 - P$ droop control is proposed for bidirectional DC-DC converters to achieve the DCV and power regulations in a DCMG. This droop approach is utilized to get rid of the negative effect of the constant power loads and to ensure a seamless transition of DCMG's operating modes. To minimize the utility cost in high electricity price condition, a decentralized control scheme is introduced by combining droop control and voltage control [18]. However, the DCV shows significant fluctuation due to the droop control in both studies. To solve this problem, a leaky integral term is implemented in the secondary control, which guarantees the DCV restoration even under event-triggered sampling [19]. In this method, the primary control is employed to maintain the current sharing via droop control in the islanded DCMG system. To improve the system robustness under uncertain parameters and enhance the power efficiency in the electric vehicle (EV), another work presents a power management strategy which integrates the droop control and disturbance observer [20]. Although these control schemes achieve their main objectives, the malfunctioned sensor device problems, which are unavoidable during the DCMG system operation, have not been mentioned.

To improve the reliability and resiliency of the overall DCMG system, it is essential to consider the failure of the sensor devices which are normally utilized to serve as the feedback signal in the controller. When the DCMG system can not identify and isolate the sensor faults, these failures give crucial effects on the stability of the overall DCMG system. Motivated by this concern, a model predictive control based on a dual-extended Kalman filter is presented for the DCMGs to detect both sensor faults and uncertain disturbances [21]. The researchers in [22] propose a fault detection and isolation (FDI) method for centralized DCMG based on an unscented Kalman filter. This control approach can apply to the nonlinear system with the minimum computing burden even under multi-sensor faults. In the study [23], another FDI strategy is used for the bidirectional DC-DC converter by applying an adaptive high-gain observer to identify various sensor failure types. In the work [24], a H_∞ observer is introduced for distributed DCMGs to estimate the voltage and current sensor value accurately. After that, a fault-tolerant control by integrating the state feedback and consensus controls is presented to maintain voltage stabilization and current sharing under sensor faults. It is worth mentioning that those FDI strategies are quite difficult to apply to the decentralized DCMG because it is more vulnerable to the sensor fault.

Inspired by these concerns, this paper presents a seamless power management for a decentralized DCMG to enhance the voltage and power stabilization under voltage sensor faults. In this study, single or multiple DCV sensor faults in the DCMG is considered. First, an observer is designed in each power agent to monitor the voltage sensor abnormality in the presence of various uncertain conditions such as the agent power variation, battery and EV SOC levels, utility grid disconnection, and high electricity prices. During the normal operations, the proposed control scheme employs the voltage droop control method with the estimated DCV value to accomplish voltage and power regulations. The voltage droop control method consists of the primary controller to guarantee the power balance and the secondary controller to maintain DCV stabilization. In addition, the droop curve of the utility grid agent is changed automatically to reduce electricity costs under the high electricity price condition. To achieve a seamless power management even under voltage sensor faults, a fault identification method is implemented for each power agent to detect voltage sensor failure based on the measured and estimated DCV values. When the power agent effectively identifies DCV sensor failure or abnormality, its operation mode is switched from the voltage droop control to the current control in order to ensure voltage stabilization as well as power balance. Compared to the previous studies, the main contributions of this paper are summarized as follows:

1) A voltage droop controller composed of the secondary controller and primary controller is deployed to regulate the DCV to the nominal value and maintain the power balance in the decentralized DCMG under uncertain conditions such as the agent power variation,

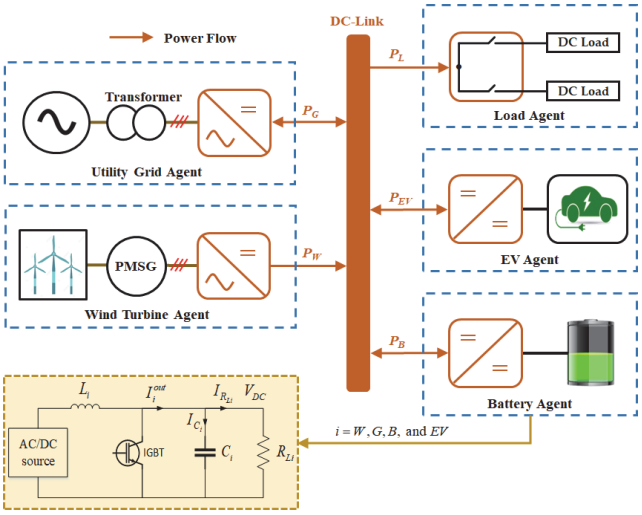

FIGURE 1. DCMG system model.

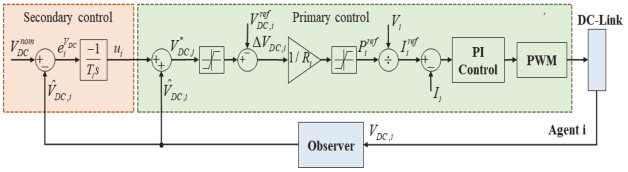

FIGURE 2. Control block diagram of the proposed control method.

battery and EV SOC levels, and utility grid disconnection. In high electricity price condition, the utility grid agent appropriately adjusts the droop curve to minimize electricity costs.

2) The proposed scheme can stably achieve the voltage regulation and power management even under simultaneous faults in several voltage sensors by virtue of a fault identification algorithm and perturbation of operating points in the droop curve, which significantly enhances the reliability of the decentralized DCMG.
3) Seamless power management can be maintained in several scenarios if only one DCV sensor works normally in the decentralized DCMG regardless of multiple DCV sensor faults by means of the proposed operation mode switching strategy.

This paper is organized as follows: Section II presents the configuration of a DCMG system considered in this study. Section III is composed of four parts, including the voltage observer of each power agent, power balance and voltage regulation based on DCV monitoring value, power management of local agents, and seamless power management under voltage sensor fault. Section IV and Section V provide the simulation and experimental results of the proposed control scheme under various test conditions, respectively. Finally, the conclusion of the paper is given in Section VI.

II. DCMG SYSTEM MODEL

Fig. 1 illustrates the system of a decentralized DCMG considered in this paper, which is composed of five power agents: a wind turbine agent, a load agent, a battery agent, an EV agent, and a utility grid agent. According to power flow, the wind turbine agent only operates in a unidirectional way to inject power to a DC-link via a unidirectional AC/DC converter and a permanent magnet synchronous generator (PMSG). In general, using a PMSG is more efficient in the wind power generation than using a doubly-fed induction generator because the power can be generated by PMSG at any speed. In decentralized DCMG, the load agent only absorbs the power from the DC-link. Based on the relationship between the supplied power and demanded power, the switches in the load agent are activated to disconnect or reconnect the load. On the other hand, the utility grid agent, battery agent, and EV agent operate in a bidirectional manner. These power agents can supply power to the DC-link or absorb excess power from the DC-link. While the utility grid agent is connected to the DCMG through the transformer and bidirectional AC/DC converter, the battery and EV agents employ the bidirectional interleaved DC/DC converter. Both the battery and EV agents absorb power from the DC-link in charging mode or inject power into the DC-link in discharging mode.

The power of the battery, EV, load, wind turbine, and utility grid agents are denoted by P_B, P_{EV}, P_L, P_W, and P_G, respectively. To clearly represent the power flow in this study, these variables have negative values $(-)$ for the injected power into the DC-link, and positive values $(+)$ for the absorbed power from the DC-link. Fig. 1 also presents the electrical structure of each power agent i consisting of a DC or AC voltage source, a converter, a capacitor C_i, and a virtual resistance R_{Li} for $i = W, G, B$, and EV in which W, G, B, and EV denote the wind turbine agent, utility grid agent, battery agent, and EV agent, respectively. It is worth mentioning that the virtual resistances are connected in parallel to satisfy the condition as

$$\sum \frac{1}{R_{Li}} = \frac{1}{R_L} \tag{1}$$

where R_L is the total load of the DCMG system. Applying Kirchhoff's current law, the dynamic model of agent i is determined as below

$$\frac{dV_{DC,i}}{dt} = -\frac{V_{DC,i}}{C_i R_{Li}} + \frac{I_i^{out}}{C_i} \tag{2}$$

where $V_{DC,i}$ is the VDC measured value from the sensor of the agent i and I_i^{out} is the converter output current of the agent i. The detailed control method and operation modes of each power agent to achieve power balance and voltage regulation even under the voltage sensor fault are presented in the subsequent sections.

III. PROPOSED CONTROL SCHEME

A. VOLTAGE OBSERVER OF EACH POWER AGENT

Fig. 2 shows a control block diagram of the proposed control scheme which is implemented in all power agents. The proposed scheme which consists of the primary control,

the secondary control, and the voltage observer, not only maintains the power balance of the DCMG system but also regulates the DCV to the nominal value even under the voltage sensor fault. In this subsection, the voltage observer is constructed to monitor the DCV value of each power agent, which serves as the only feedback signal from the DC-link to the agent i in the absence of DCLs in the DCMG system. When all the DCV sensors of the DCMG system operate properly, each power agent correctly estimates the DCV value by using the DCV measurement, the converter output current, and modeling parameters. If a fault occurs in one of the DCV sensors in the DCMG system, the power agent including this faulted sensor can effectively identify the occurrence of this fault by the discrepancy between the measured and estimated DCV values. Once the fault is detected, the operating mode of each power agent is explicitly specified to prevent the system collapse due to the power imbalance. The detailed detection method and operation mode of each power agent are presented in Subsection III-D.

A voltage observer of power agent i is constructed as

$$\dot{\hat{V}}_{DC,i} = -\frac{1}{C_i R_{Li}}\hat{V}_{DC,i} + \frac{1}{C_i} I_i^{out} + L_i\left(V_{DC,i} - \hat{V}_{DC,i}\right) \quad \text{for } i = W, G, B, \text{ and } EV \tag{3}$$

where the symbol "$\wedge$" denotes the estimated variables and L_i is the observer gain. If the estimation error is defined as $e_i(t) = V_{DC,i} - \hat{V}_{DC,i}$, the error dynamic is calculated as follows:

$$\dot{e}_i(t) = -\left(\frac{1}{C_i R_{Li}} + L_i\right) e_i(t). \tag{4}$$

The overall system dynamic can be obtained as follow:

$$\dot{e} = Ke \tag{5}$$

where $K = diag(K_B, K_{EV}, K_G, K_W)$ $\forall K_i = -\left(\frac{1}{C_i R_{Li}} + L_i\right)$ $e = [e_B, e_{EV}, e_G, e_W]^T$. For the overall system to be stable, L_i of each agent is chosen to satisfy that K is a Hurwitz matrix.

To enhance the reliability and resiliency of the decentralized DCMG system, this study takes into account several uncertain conditions such as agent power variation, the battery and EV SOC levels, utility grid disconnection, and high electricity price conditions. The detailed control method of each power agent to maintain power and voltage regulation even under uncertain conditions is outlined in the next subsection.

B. POWER BALANCE AND VOLTAGE REGULATION BASED ON DCV MONITORING VALUE

In this subsection, the secondary controller and primary controller to ensure both voltage stabilization and optimal power management are presented based on the DCV monitoring value as shown in Fig. 2. While the power balance is achieved by V-P droop curves in the primary controller [18], the secondary controller is utilized to maintain the DCV at the nominal value [25]. The voltage restoration error $e_i^{V_{DC}}$ between the nominal DCV V_{DC}^{nom} and estimated DCV $\hat{V}_{DC,i}$ is defined as

$$e_i^{V_{DC}} = V_{DC}^{nom} - \hat{V}_{DC,i}. \tag{6}$$

Then, the DCV compensator u_i can be obtained by using an integral term as

$$\dot{u}_i = -\frac{e_i^{V_{DC}}}{T_i} \tag{7}$$

where T_i is an integrator gain. The auxiliary variable $V_{DC,i}^*$, which is used to determine the operation mode of agent i in the primary control, is determined as

$$V_{DC,i}^* = \hat{V}_{DC,i} + u_i. \tag{8}$$

The auxiliary variable $V_{DC,i}^*$ can be used in the primary controller as follows:

$$V_{DC,i}^* = V_{DC,i}^{ref} + R_i P_i^{ref}, \text{ for } i = W, G, B, \text{ and} EV \tag{9}$$

where $V_{DC,i}^{ref}$, R_i, and P_i^{ref} are the DCV reference, the droop characteristic, and the power reference of agent i, respectively. The power reference P_i^{ref} of agent i can be obtained based on the selection of $V_{DC,i}^{ref}$ and the droop characteristic R_i as follows:

$$P_i^{S,max} \le P_i^{ref} \le P_i^{C,max}$$
$$V_{DC,i}^{*,L} \le V_{DC,i}^* \le V_{DC,i}^{*,H} \tag{10}$$

$$R_i = \frac{\Delta V_{DC,i}}{\Delta P_i} = \frac{V_{DC,i}^{*,H} - V_{DC,i}^{*,L}}{P_i^{C,max} - P_i^{S,max}} \tag{11}$$

where $V_{DC,i}^{*,L}$, $V_{DC,i}^{*,H}$, $P_i^{C,max}$, and $P_i^{S,max}$ are the low voltage level, the high voltage level, the maximum consumed power, and the maximum supplied power of agent i, respectively. The current reference I_i^{ref} is determined as $I_i^{ref} = P_i^{ref}/V_i$ with V_i as the voltage of the power agent i. Then, the current error is processed by the proportional-integral (PI) current controller of the power agent i. The PI current control gains in the power agent i are selected in order that the current control has faster dynamic response than the droop controller within the primary controller.

As mentioned earlier, the main objective of the secondary control is to ensure the regulation of the DCV to the nominal value. For this aim, the integrator gain T_i, auxiliary variable $V_{DC,i}^*$, and the nominal DCV V_{DC}^{nom} of each power agent should be identical according to earlier work [19], [25]. On the other hand, the values of $V_{DC,i}^{*,L}$, $V_{DC,i}^{*,H}$, $P_i^{C,max}$, and $P_i^{S,max}$ should be established initially as in earlier work [25]. To construct a voltage observer by (3) in the proposed control scheme, the converter output current of the agent i I_i^{out} is determined as follows:

$$I_i^{out} = \frac{-P_i^{ref}}{\hat{V}_{DC,i}} \tag{12}$$

In this study, several uncertain conditions such as agent power variation, the battery and EV SOC levels, utility

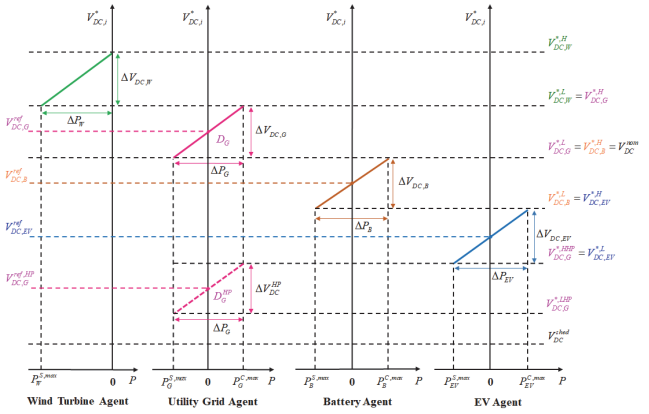

FIGURE 3. V* - P droop curves for DCMG system.

grid disconnection, and high electricity price conditions are considered. These uncertain conditions make the virtual resistance of each power agent R_{Li} vary according to the converter power of each agent (P_i). To construct a voltage observer by (3) in the proposed control scheme, the virtual resistance of power agent i, R_{Li} is determined as follows:

$$R_{Li} = \begin{cases} R_{Li}^{\max} & \forall P_i \in [-\gamma, 0] \\ -\dfrac{\hat{V}_{DC,i}^2}{P_i} & \forall P_i \in \left\{\left[P_i^{S,\max}, -\gamma\right] \cup \left[\gamma, P_i^{C,\max}\right]\right\} \\ -R_{Li}^{\max} & \forall P_i \in [0, \gamma] \end{cases} \tag{13}$$

where γ is a small positive value, $R_{Li}^{\max}$ is the maximum value of the virtual resistance. In the above equations, γ is used to avoid the value of R_{Li} from being infinite when the power of agent i approaches zero.

C. POWER MANAGEMENT OF LOCAL AGENTS IN DCMG SYSTEM

Fig. 3 shows $V^* - P$ droop curves for the DCMG system which achieve optimal power management both in the grid-connected and islanded modes when there are no voltage sensor faults. The auxiliary variable $V_{DC,i}^*$ is employed to determine the operation mode of agent i in the primary control. Without voltage sensor fault, the $V_{DC,i}^*$ values from the secondary controller in all power agents are identical. Thus, the operation mode of each power agent is determined in the primary controller by using individual $V_{DC,\,i}^{ref}$ and R_i which are obtained from $V_{DC,\,i}^{*,L}$ and $V_{DC,\,i}^{*,H}$. In this study, the droop characteristic of agent i (R_i) which indicates the inclination of the voltage droop is determined in (11) based on $V_{DC,\,i}^{*,L}$, $V_{DC,\,i}^{*,H}$, $P_i^{C,max}$, and $P_i^{S,max}$ without considering any deadband as earlier works [18], [25].

As shown in Fig. 3, in case of the normal electricity price condition, the values of $V_{DC,\,i}^{*,L}$ and $V_{DC,\,i}^{*,H}$ of each power agent are selected based on the priority order for energy support to the DC-link as follows: the wind turbine agent, utility grid agent, battery agent, and EV agent. In contrast, under the high electricity price condition, the priority order for energy support to the DC-link is given as the wind turbine agent, battery agent, EV agent, and utility grid agent.

TABLE 1. Operation modes of each power agent in DCMG system.

Power agent	Description	Operating modes
Utility grid agent	Utility grid disconnection	DIS
	Utility grid current control mode	GCCM
	Utility grid droop control by the inverter mode	INV
	Utility grid droop control by the converter mode	CON
Battery agent	Idle mode	IDLE
	Battery current control mode	BCCM
	Battery droop control by the discharging mode	BDDM
	Battery droop control by the charging mode	BDCM
EV agent	Idle mode	IDLE
	EV current control mode	ECCM
	EV droop control by the discharging mode	EDDM
	EV droop control by the charging mode	EDCM
Wind turbine agent	Maximum power point tracking mode	MPPT
	Wind turbine current control mode	WCCM
	Wind turbine droop control mode	WDCM
Load agent	Load shedding	LS
	Load reconnecting	LR
	Load under a normal condition	Normal

Table 1 presents the operation modes of each power agent in the decentralized DCMG system. The detailed operation modes of each power agent are explained without voltage sensor fault.

1) ISLANDED MODE

When $V_{DC,\,i}^*$ is in the region between the low voltage level $V_{DC,\,W}^{*,L}$ and the high voltage level $V_{DC,\,W}^{*,H}$ of the wind turbine agent, it indicates that the generated power of the wind turbine agent exceeds the sum power of P_L, the maximum consumed power of the battery agent ($P_B^{C,max}$), and maximum consumed power of the EV agent ($P_{EV}^{C,max}$). To maintain the voltage stabilization and power balance in decentralized DCMG, the wind turbine agent operates in the wind turbine droop control mode (WDCM) in Table 1 to regulate the DCV to the nominal value. In this case, the battery and EV agents operate in BDCM and EDCM with $P_B^{C,max}$ and $P_{EV}^{C,max}$, respectively.

If $V_{DC,\,i}^*$ is located between the low voltage level $V_{DC,\,B}^{*,L}$ and the high voltage level $V_{DC,\,B}^{*,H}$ of the battery agent, it means that the wind turbine agent injects power less than the sum of the demand load and maximum battery and EV charging powers. In this case, the battery agent regulates DCV via the droop control method using the estimated DCV value, and manages the power inside the DCMG system to ensure the power balance. When $V_{DC,i}^*$ is higher than the DCV reference value of the battery agent $V_{DC,\,B}^{ref}$ and the battery SOC (SOC_B) is not full, the battery agent operates in BDCM to absorb power from the DC-link. Otherwise, the battery agent supplies power to the DC-link through BDDM unless SOC_B approaches the lowest value. In both situations, the wind turbine agent operates in MPPT modes to inject the

maximum power, whereas the EV agent absorbs the power from the DC-link with $P_{EV}^{C,max}$ via EDCM.

Once $V_{DC,\,i}^{*}$ is in the region between the low voltage level $V_{DC,\,EV}^{*,L}$ and the high voltage level $V_{DC,\,EV}^{*,H}$ of the EV agent, and the sum of the maximum supporting power of the wind turbine agent ($P_{W}^{S,max}$) and maximum supporting power of the battery agent ($P_{B}^{S,max}$) is less than the sum of P_L and $P_{EV}^{C,max}$, the EV agent controls DCV to the nominal value. Similar to the battery agent, the EV agent operates in EDCM when $V_{DC,i}^{*}$ is higher than the DCV reference value of the EV agent $V_{DC,\,EV}^{ref}$ and the EV SOC (SOC_E) is not full. As $V_{DC,i}^{*}$ is less than $V_{DC,\,EV}^{ref}$ and SOC_E is not the lowest value, the EV agent supplies power to the DC-link by EDDM to maintain the power balance. In these cases, both wind turbine and battery agents supply the maximum power to the DC-link by MPPT and BDDM, respectively.

When the load demand exceeds the sum of the maximum supplied power by the wind turbine, battery, and EV agents, it causes $V_{DC,\,i}^{*}$ to reduce significantly. As soon as $V_{DC,\,i}^{*}$ drops to the load shedding voltage level V_{DC}^{shed}, the load shedding mode is activated based on the load priority to avoid the collapse of the DCMG system as mentioned in the earlier work [22]. As $V_{DC,\,i}^{*}$ reaches to V_{DC}^{nom}, the load reconnecting mode is immediately activated.

2) GRID-CONNECTED MODE

In this situation, the utility grid agent regulates DCV to the nominal value via the droop control method using the estimated DCV value to achieve voltage regulation and power balance. Based on the electricity price condition, the utility grid agent adjusts the $V^{*}-P$ droop curve to reduce utility costs.

In case of the normal electricity price condition of the grid-connected mode without voltage sensor fault, the utility grid agent achieves voltage regulation in decentralized DCMG. In this situation, $V_{DC,\,i}^{*}$ lies in the region between the low voltage level $V_{DC,\,G}^{*,L}$ and the high voltage level $V_{DC,\,G}^{*,H}$ in the normal electricity price condition of the utility grid agent. As a result, the utility grid agent regulates DCV to the nominal value with the droop curve in the normal electricity price condition (D_G) as shown in Fig. 3. The wind turbine agent operates in MPPT mode to inject the maximum power, and the battery and EV agents absorb the maximum power from the DC-link through BDCM and EDCM, respectively. When the generated power of the wind turbine agent exceeds the sum of P_L, $P_{B}^{C,max}$, and $P_{EV}^{C,max}$, $V_{DC,i}^{*}$ is higher than the DCV reference value in the normal electricity price condition of the utility grid agent ($V_{DC,\,G}^{ref}$). In this case, the utility grid agent operates in INV mode to absorb the power from the DC-link. Otherwise, the utility grid agent supplies power to the DC-link by CON mode to ensure the power balance.

When the utility grid condition is changed to the high electricity price, the $V^{*}-P$ droop curve of the utility grid agent is automatically changed to the droop curve in the high electricity price condition (D_G^{HP}) to minimize the utility costs as shown in Fig. 3. In this situation, the utility grid agent absorbs power from the DC-link as much as possible. According to the droop curve D_G^{HP} of the utility grid agent, the $V_{DC,\,i}^{*}$ value is located in the region between the low voltage level $V_{DC,\,G}^{*,LHP}$ and the high voltage level $V_{DC,\,G}^{*,HHP}$ in the high electricity price condition of the utility grid agent. The wind turbine, battery, and EV agents supply the maximum power to the DC-link via MPPT, BDDM, and EDDM, respectively. Once the load demand is less than the sum of the generated power of $P_{W}^{S,max}$, $P_{B}^{S,max}$, and the maximum supporting power of the EV agent ($P_{EV}^{S,max}$), it causes $V_{DC,i}^{*}$ to be higher than the DCV reference value in the high electricity price condition of the utility grid agent ($V_{DC,\,G}^{ref,HP}$) in the droop curve D_G^{HP}. Then, the utility grid agent operates in INV mode to regulate DCV to the nominal value. When the load demand is more than the sum of the maximum supply power of the wind turbine, battery, and EV agents, $V_{DC,i}^{*}$ is reduced less than $V_{DC,\,G}^{ref,HP}$ of the droop curve D_G^{HP}. Then, the utility grid agent switches the operation from INV mode to CON mode even under the high electricity price condition to avoid the power imbalance and voltage fluctuation of the DCMG system.

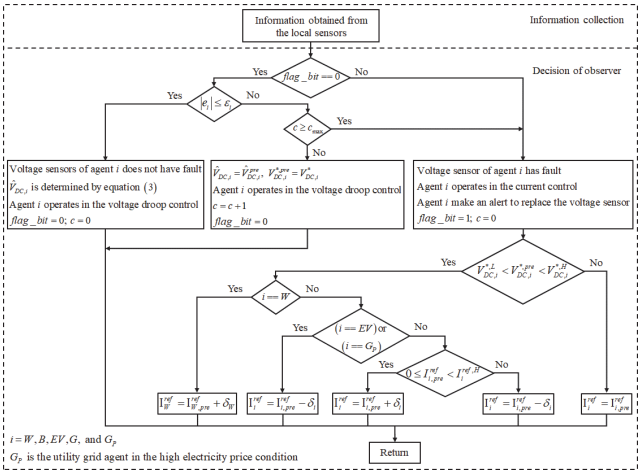

FIGURE 4. Voltage sensor fault identification and operation mode decisions of agent i under voltage sensor fault.

D. SEAMLESS POWER MANAGEMENT UNDER VOLTAGE SENSOR FAULT

In the previous subsection, optimal power management of the DCMG system has been presented to minimize the utility costs by shifting the droop curve of the utility grid agent. To enhance the reliability of the decentralized DCMG system, seamless power management in the presence of voltage sensor faults is presented.

Fig. 4 shows the voltage sensor fault identification and operation mode decisions of each power agent in the decentralized DCMG under the DCV sensor fault. In this figure, c, $c_{\max}$, $\hat{V}_{DC,i}^{pre}$, and $V_{DC,i}^{*,pre}$ denote the counter of agent i, the maximum value of c, the estimated DCV value in the previous time step, and the auxiliary variable in the previous time step.

In addition, ε_i is the threshold voltage value of the power agent i as in the earlier work [23]. The internal variable in each power agent i (*flag_bit*) is utilized to determine whether the power agent i has the DCV sensor fault. The variable *flag_bit* set to one indicates that there exists a voltage sensor fault in the power agent i. In contrast, if the variable *flag_bit* equals zero, it indicates that the DCV sensor of the power agent i works correctly.

When *flag_bit* of agent i equals zero, the voltage sensor fault identification algorithm is activated to monitor the sensor abnormality by using the estimation error e_i between $V_{DC,i}$ and $\hat{V}_{DC,i}$. If the absolute value of e_i is less than ε_i, it represents that the DCV sensor of the power agent i works correctly. Then, the power agent i operates normally in the voltage droop method, in which the detailed operation modes of each power agent are determined as explained in Subsection III-C. As $|e_i|$ is larger than ε_i caused by DCV sensor failure or abnormality, the counter c is used to count this event. If c is lower than $c_{\max}$ with $|e_i| > \varepsilon_i$, the timer counter c is increased, and power agent i continues to operate in the voltage droop method with the estimated DCV value of agent i, $\hat{V}_{DC,i}$ set to $\hat{V}^{pre}_{DC,i}$ before $|e_i| > \varepsilon_i$. However, once c is increased higher than $c_{\max}$, the power agent i recognizes that the DCV voltage sensor has a fault. Then, the power agent i immediately set *flag_bit* to one, and switches the operation mode from the voltage droop control method to the PI current control method to maintain the DCMG system stability. After the DCV sensor fault is identified, the current reference I^{ref}_i of the PI current control in power agent i is established by using the auxiliary variable before the voltage sensor fault ($V^{*,pre}_{DC,i}$) to achieve seamless power management of the decentralized DCMG system.

1) CASE 1 ($V^{*,pre}_{DC,i} < V^{*,L}_{DC,i}$) OR ($V^{*,pre}_{DC,i} > V^{*,H}_{DC,i}$)

When $V^{*,pre}_{DC,i}$ is lower than $V^{*,L}_{DC,i}$ or $V^{*,pre}_{DC,i}$ is higher than $V^{*,H}_{DC,i}$, it indicates that the power agent i did not regulate the DCV before the DCV sensor fault occurred. In this case, to maintain the power balance of the DCMG system, the power agent i operates in the current control mode with the current reference determined as

$$\mathrm{I}^{ref}_i = \mathrm{I}^{ref}_{i,pre} \tag{14}$$

where $I^{ref}_{i,pre}$ is the current reference of the power agent i before the DCV sensor fault occurs. It is worth mentioning that other power agents in the DCMG can not recognize whether the power agent i has the DCV sensor fault because of lack of communication data among power agents in the decentralized control method. Hence, an alert to other power agents is necessary to replace the voltage sensor or to reconfigure the decentralized DCMG system.

2) CASE 2 ($V^{*,L}_{DC,i} < V^{*,pre}_{DC,i} < V^{*,H}_{DC,i}$)

When $V^{*,pre}_{DC,i}$ is in the region between $V^{*,L}_{DC,i}$ and $V^{*,H}_{DC,i}$, it means the power agent i regulated the DCV to the nominal value before the voltage sensor fault. Because the power agent i changes the operation mode from the voltage droop control method to the PI current control as a result of the DCV sensor fault, no power agents in the decentralized DCMG system regulate the DCV. To achieve a seamless power management and voltage regulation even in this circumstance, the power agent i assigns I^{ref}_i of the PI current control properly to orientate $V^{*}_{DC,i}$ to the different voltage range $\left[V^{*,L}_{DC,i}, V^{*,H}_{DC,i}\right]$, in order that other agents can regulate the DCV. In this situation, one of the power agents in the decentralized DCMG, which does not have the DCV sensor fault, can regulate the DCV to the nominal value.

In the islanded mode, if the fault occurs in the DCV sensor of the wind turbine agent and $V^{*}_{DC,i}$ (for $i = W$) is in the region between $V^{*,L}_{DC,W}$ and $V^{*,H}_{DC,W}$, the wind turbine agent changes the operation mode from the WDCM to the wind turbine PI current control mode (WCCM) with the current reference I^{ref}_W set as follows:

$$I^{ref}_W = I^{ref}_{W,pre} + \delta_W \tag{15}$$

where δ_W and $I^{ref}_{W,pre}$ are the positive value and the current reference before the DCV sensor fault of the wind turbine agent occurred. Adding δ_W to $I^{ref}_{W,pre}$ causes the supplied power to the DC-link by the wind turbine agent to be reduced before the instant of the voltage sensor fault. As a result, the $V^{*}_{DC,i}$ is decreased continuously to $V^{*,H}_{DC,B}$, in which the battery agent can take a control of the DCV to ensure voltage stabilization.

In the islanded mode, if the DCV sensor fault occurs in the EV agent and $V^{*}_{DC,i}$ (for $i = EV$) is in the region between $V^{*,L}_{DC,EV}$ and $V^{*,H}_{DC,EV}$, the operation mode of the EV agent is switched from the EV voltage droop control mode (EDDM or EDCM) to the EV current control mode (ECCM) with the EV current reference I^{ref}_{EV} chosen as follows:

$$I^{ref}_{EV} = I^{ref}_{EV,pre} - \delta_{EV} \tag{16}$$

where δ_{EV} and $I^{ref}_{EV,pre}$ are the positive value and the current reference before the DCV sensor fault occurred in the EV agent. Negative current introduced by δ_{EV} in (16) increases $V^{*}_{DC,i}$. If the EV agent is working as charging mode before the instant of the voltage sensor fault, (16) reduces EV absorbing power. On the contrary, if the EV agent is working as discharging mode before the instant of the voltage sensor fault, (16) increases supplied EV power. As $V^{*}_{DC,i}$ reaches to $V^{*,L}_{DC,B}$, the battery agent can regulate the DCV to the nominal value.

Finally, in the islanded mode, when the battery agent regulates the DCV before its voltage sensor fault and $V^{*}_{DC,i}$ (for $i = B$) is in the region between $V^{*,L}_{DC,B}$ and $V^{*,H}_{DC,B}$, the battery current reference I^{ref}_B can be obtained by using the highest battery current reference ($I^{ref,H}_{B,pre}$) and the battery current reference ($I^{ref}_{B,pre}$) before the DCV sensor fault. As $I^{ref}_{B,pre}$ is higher than zero and lower than $I^{ref,H}_B$, I^{ref}_B in the battery

current control mode (BCCM) is set as $I_B^{ref} = I_{B,pre}^{ref} + \delta_B$ with δ_B being a positive value. In this situation, the battery agent absorbs more power from the DC-link before its DCV sensor fault, which causes $V_{DC,\,i}^{*}$ to drop. When $V_{DC,\,i}^{*}$ decreases below $V_{DC,\,EV}^{*,H}$, the EV agent can take a control of the DCV to maintain voltage regulation. In contrast, if $I_{B,pre}^{ref}$ is not in the region between zero and $I_B^{ref,H}$, the battery agent operates in BCCM mode with I_B^{ref} set as $I_B^{ref} = I_{B,pre}^{ref} - \delta_B$. In this case, $V_{DC,\,i}^{*}$ is increased continuously because the battery agent supplies more power to the DC-link before the DCV sensor fault occurs. As $V_{DC,\,i}^{*}$ reaches to $V_{DC,\,W}^{*,L}$, the wind turbine agent can regulate the DCV to the nominal value.

As the decentralized DCMG operates in the grid-connected mode with the normal electricity price condition, the utility grid agent regulates DCV to the nominal value with the droop curve D_G. A sudden DCV sensor fault of the utility grid agent causes its operation mode to switch from the utility grid voltage droop mode (INV or CON) to the utility grid current control mode (GCCM). Similar to the condition of the battery DCV sensor fault, if the utility grid current reference ($I_{G,pre}^{ref}$) before the DCV sensor fault is in the region between zero and the highest utility grid current reference ($I_{G,pre}^{ref,H}$), the utility grid current reference I_G^{ref} is set to $I_G^{ref} = I_{G,pre}^{ref} + \delta_G$ with a positive value of δ_G. Otherwise, I_G^{ref} is chosen as $I_G^{ref} = I_{G,pre}^{ref} - \delta_G$ if $I_{G,pre}^{ref}$ is less than zero. In both situations, other agents in the decentralized DCMG regulate the DCV according to the $V_{DC,\,i}^{*}$ value.

In the high electricity price condition, the DCV is regulated according to the droop curve D_G^{HP}. If a fault occurs in the utility grid DCV sensor, the operation mode of the utility grid agent is immediately switched to GCCM. Similar to the condition of the DCV sensor fault in EV, the utility grid current reference I_G^{ref} is set to $I_G^{ref} = I_{G,pre}^{ref} - \delta_G$, which causes $V_{DC,\,i}^{*}$ to increase. As $V_{DC,\,i}^{*}$ is higher than $V_{DC,\,EV}^{*,L}$, the EV agent regulates the DCV to maintain the DCMG system stability.

IV. SIMULATION RESULTS

In this section, the simulations are conducted for a decentralized DCMG to demonstrate the feasibility and reliability of the proposed control scheme based on the PSIM software. Simulation results are presented in several uncertain conditions, including the voltage sensor fault, high electricity price condition, agent power variation, utility grid disconnection, and the different SOC levels of the battery and EV agents with the system parameters listed in Table 2.

TABLE 2. System parameters of a decentralized DCMG system.

Power agent	Parameters	Symbol	Value
Utility grid agent	Grid voltage	V_G^{rms}	220 V
	Grid frequency	f_G	60 Hz
	Maximum consuming power	$P_G^{C,max}$	2000 W
	Maximum supporting power	$P_G^{S,max}$	−2000 W
	High voltage level in normal electricity price	$V_{DC,\,G}^{*,H}$	410 V
	Low voltage level in normal electricity price	$V_{DC,\,G}^{*,L}$	400 V
	High voltage level in high electricity price	$V_{DC,\,G}^{*,HHP}$	380 V
	Low voltage level in high electricity price	$V_{DC,\,G}^{*,LHP}$	370 V
	Utility grid threshold voltage value	ε_G	6 V
Wind turbine agent	PMSG number of poles	p	6
	PMSG inertia	J	0.11 kgm^2
	PMSG flux linkage	ψ	0.18 Wb
	Maximum supporting power	$P_W^{S,max}$	−1500 W
	High voltage level	$V_{DC,\,W}^{*,H}$	415 V
	Low voltage level	$V_{DC,\,W}^{*,L}$	410 V
	Wind turbine threshold voltage value	ε_W	6 V
Battery agent	Maximum battery SOC	$SOC_{max,\,B}$	90 %
	Minimum battery SOC	$SOC_{min,\,B}$	20 %
	Maximum battery voltage	V_B^{max}	180 V
	Maximum consuming power	$P_B^{C,max}$	540 W
	Maximum supporting power	$P_B^{S,max}$	−540 W
	High voltage level	$V_{DC,\,B}^{*,H}$	400 V
	Low voltage level	$V_{DC,\,B}^{*,L}$	390 V
	Battery threshold voltage value	ε_B	6 V
EV agent	Maximum EV SOC	$SOC_{max,\,EV}$	90 %
	Minimum EV SOC	$SOC_{min,\,EV}$	20 %
	Maximum EV voltage	V_{EV}^{max}	180 V
	Maximum consuming power	$P_{EV}^{C,max}$	360 W
	Maximum supporting power	$P_{EV}^{S,max}$	−360 W
	High voltage level	$V_{DC,\,EV}^{*,H}$	390 V
	Low voltage level	$V_{DC,\,EV}^{*,L}$	380 V
	EV threshold voltage value	ε_{EV}	6 V
Load agent	Load 1	R_{L1}	800 Ω
	Load 2	R_{L2}	800 Ω
	Load 3	R_{L3}	800 Ω
	Priority level: load 1 > load 2 > load 3	-	-
DC bus	Load shedding voltage level	V_{dc}^{shed}	360 V
	Nominal voltage	V_{dc}^{nom}	400 V

A. TRANSITION BETWEEN GRID-CONNECTED MODE AND ISLANDED MODE WITHOUT DCV SENSOR FAULT

Fig. 5 shows the simulation results for the transition between the grid-connected mode and islanded mode without voltage sensor fault. It is assumed that the DCMG system starts in the islanded mode, SOC_B is at the lowest level while SOC_{EV} is in the region [$SOC_{min,EV}$, $SOC_{max,EV}$]. Because the wind turbine agent supplies power lower than the demand load, the EV agent regulates DCV to V_{DC}^{nom} via EDDM, and $V_{DC,\,i}^{*}$ is in the range of $\left[V_{DC,\,EV}^{*,L}, V_{DC,\,EV}^{*,H}\right]$. In this situation, the wind turbine and battery agents operate in the MPPT and IDLE modes, respectively.

Once the wind turbine power suddenly falls at $t = 0.4$ s, $V_{DC,i}^{*}$ drops rapidly because the sum of wind turbine power generation and the maximum EV discharging power is less

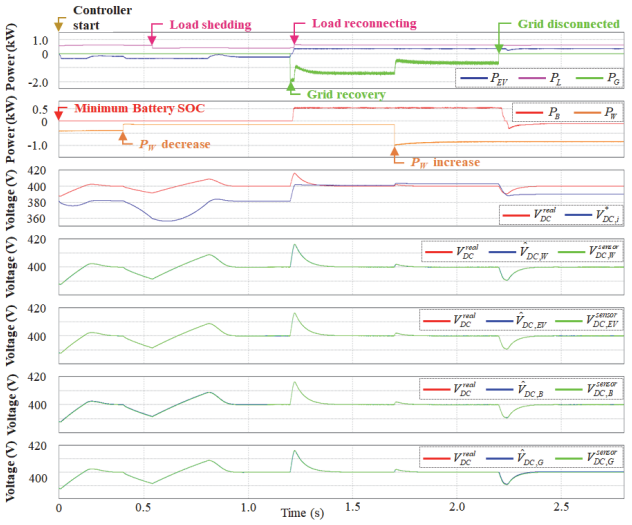

FIGURE 5. Simulation results for the transition between islanded mode and grid-connected mode without voltage sensor fault.

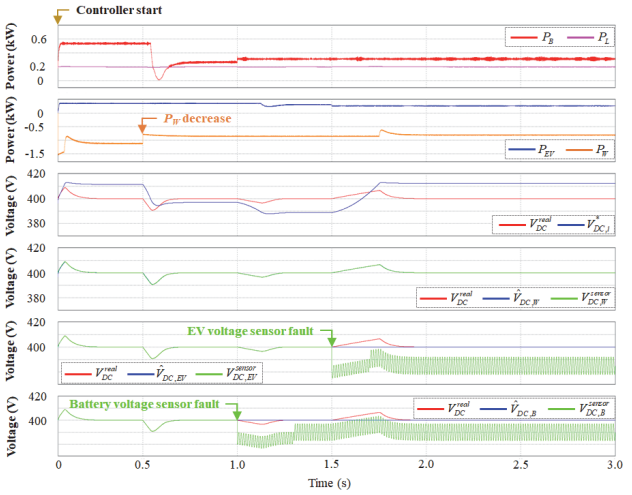

FIGURE 6. Simulation results for the islanded mode under voltage sensor faults.

than the load demand. To avoid the power imbalance, the load shedding mode is activated as soon as $V^{*}_{DC,i}$ falls to V^{shed}_{DC}. As a result of load shedding, $V^{*}_{DC,i}$ increases beyond $V^{*,L}_{DC,\,EV}$. Thus, the EV agent continues regulating DCV at V^{nom}_{DC} via EDDM mode while the wind turbine and battery agents still work in MPPT and IDLE modes, respectively.

When the utility grid agent is recovered from the fault with the normal electricity price condition at $t = 1.2$ s, the utility grid agent operates in the CON mode based on the droop curve D_G to supply power to the DC-link. In addition, the load reconnecting is activated because $V^{*}_{DC,i}$ lies in the region between $V^{*,L}_{DC,\,G}$ and $V^{*,H}_{DC,\,G}$. The battery and EV agents switch the operation mode from IDLE and EDDM to BDCM and EVDM, respectively, while the wind turbine agent continues operating in MPPT mode. Although the wind turbine agent supplies more power to the DC-link at $t = 1.7$ s, the sum power of P_L, $P^{C,max}_{B}$, and $P^{C,max}_{EV}$ exceeds the wind turbine power generation. In this situation, all power agents in the decentralized DCMG do not change the operation mode.

As the grid fault occurs without voltage sensor fault at $t = 2.2$ s, the decentralized DCMG system is changed to the islanded mode. Because the wind turbine agent injects power less than the sum of the demand load and maximum EV charging powers, $V^{*}_{DC,\,i}$ decreases below $V^{ref}_{DC,\,B}$. As a result, the operation mode of battery agent is changed from BDCM to BDDM to ensure the DCV stabilization. The wind turbine and EV agents still operate in MPPT and EDCM modes, respectively. It can be seen from Fig. 5 that the estimated DCV value $\hat{V}_{DC,i}$ tracks $V_{DC,i}$ accurately regardless of utility grid disconnection and agent power variation. Also, it is shown that the power balance and voltage regulation are achieved by the proposed control scheme even under such uncertain conditions.

B. ISLANDED MODE UNDER VOLTAGE SENSOR FAULTS

To verify a seamless power management of the proposed scheme, Fig. 6 shows the simulation results in the islanded mode under voltage sensor faults. Similarly, all the agents start in the islanded mode without DCV sensor fault. Both SOC_B and SOC_{EV} are in the region between the minimum and maximum SOC levels. Because the generated power by the wind turbine agent exceeds the sum of P_L, $P^{C,max}_{B}$, and $P^{C,max}_{EV}$, the wind turbine agent operates in WDCM mode to regulate the DCV to the nominal value, and $V^{*}_{DC,\,i}$ lies in the range of $\left[V^{*,L}_{DC,\,W}, V^{*,H}_{DC,\,W}\right]$. In this case, the battery and EV agents operate in BDCM and EDCM with the maximum charging power $P^{C,max}_{B}$ and $P^{C,max}_{EV}$, respectively.

When the wind turbine power suddenly falls at $t = 0.5$ s, it causes $V^{*}_{DC,\,i}$ to decrease continuously. As soon as $V^{*}_{DC,\,i}$ drops to $V^{*,H}_{DC,\,B}$, the battery agent decreases the absorbing power from the DC-link to ensure the power balance. In this situation, the operation mode of the wind turbine agent is changed from WDCM to MPPT mode to inject the maximum power while the EV agent still absorbs the maximum power via EDCM.

At $t = 1.0$ s, when the battery agent regulates the DCV via BDCM mode, the fault occurs in the DCV sensor of the battery agent. First, the battery agent identifies its DCV sensor fault by the fault identification algorithm using the estimated DCV in Fig. 4. Then, the battery agent switches the operation mode from the BDCM to the BCCM with $I^{ref}_{B} = I^{ref}_{B,pre} + \delta_B$. In this case, the battery agent absorbs more power from the DC-link before the instant of its DCV sensor fault, which causes $V^{*}_{DC,\,i}$ to decrease. As $V^{*}_{DC,\,i}$ drops to $V^{*,H}_{DC,\,EV}$, the EV agent can regulate the DCV to the nominal value through EDCM while the operation mode of the wind turbine agent is kept in MPPT mode.

At $t = 1.5$ s the DCV sensor of the EV agent also has a sudden fault. Then, the EV agent changes the operation mode

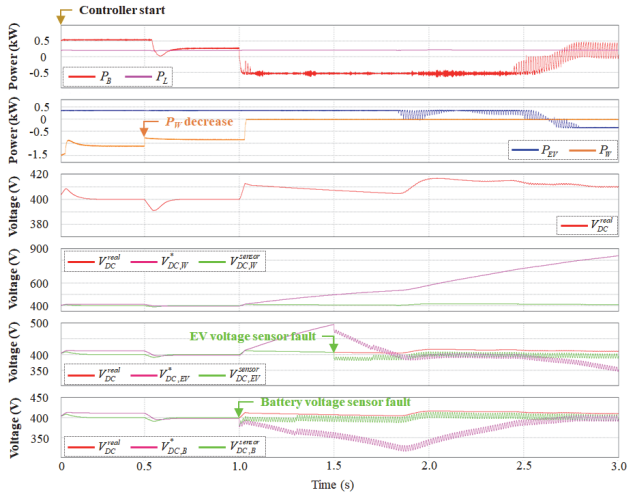

FIGURE 7. Simulation results for the islanded mode under voltage sensor faults by the scheme in [25].

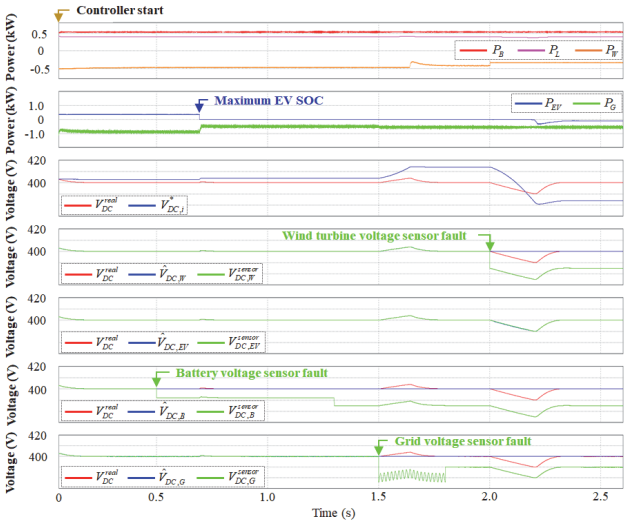

FIGURE 8. Simulation results for the grid-connected mode under voltage sensor faults.

from EDCM to ECCM with I_{EV}^{ref} given in (16). This causes $V_{DC,\,i}^{*}$ to reach to $V_{DC,\,W}^{*,L}$ because the EV agent decreases the absorbing power from the DC-link. In this situation, the wind turbine agent operates in WDCM mode to maintain the voltage stabilization while both the battery and EV agents work in BCCM and ECCM, respectively.

To emphasize the effectiveness and reliability of the proposed control scheme, Fig. 7 shows the simulation results of the method [25] under voltage sensor faults in the islanded mode. When the decentralized DCMG system is faced with DCV sensor fault at $t = 1.0$ s, the voltage and power of each agent in the decentralized DCMG are extremely unstable. In Fig. 7, the power imbalance and voltage fluctuation are clearly observed when the DCV sensor has faults. Because $V_{DC,\,W}^{*}$, $V_{DC,\,EV}^{*}$, and $V_{DC,\,B}^{*}$ are not identical, power agents can not determine their operation modes properly as in the study [25]. In particular, the wind turbine power approaches zero after 1.0 s because $V_{DC,\,W}^{*}$ exceeds $V_{DC,\,W}^{*,H}$. The powers from the EV and battery agents are also fluctuating severely, which causes a negative impact on the converter and battery SOC lifetime.

C. GRID-CONNECTED MODE IN NORMAL ELECTRICITY PRICE UNDER DCV SENSOR FAULTS

To emphasize an uninterruptable power management of the proposed scheme, Fig. 8 shows the simulation results for the grid-connected DCMG in the normal electricity price condition under voltage sensor faults. The DCMG system starts in the grid-connected mode with both SOC_B and SOC_{EV} in the region between the minimum and maximum SOC levels. Because the generated power of the wind turbine agent is less than the sum of P_L, $P_B^{C,max}$, and $P_{EV}^{C,max}$, the utility grid agent operates in CON mode to supply the power to the DC-link with $V_{DC,i}^{*}$ lying in the region $\left[V_{DC,\,G}^{*,L},\, V_{DC,\,G}^{*,H}\right]$. In this case, the wind turbine, battery, and EV agents operate in the MPPT, BDCM, and EDCM, respectively.

At $t = 0.5$ s, the DCV sensor fault occurs in the battery agent with $V_{DC,i}^{*}$ being in the region $\left[V_{DC,\,G}^{*,L},\, V_{DC,\,G}^{*,H}\right]$. Then, the battery agent switches the operation mode from the BDCM to the BCCM with $I_B^{ref} = I_{B,pre}^{ref}$ as in (14). In this situation, the EV, utility grid, and wind turbine agents keep in EDCM, CON, and MPPT modes, respectively. It is shown from this test that the power balance is ensured in spite of the DCV sensor fault of the battery agent in the grid-connected mode. When SOC_{EV} reaches to $SOC_{max,EV}$ at $t = 0.7$ s, the EV agent switches to IDLE mode.

If another DCV sensor failure occurs in the utility grid agent at $t = 1.5$ s, the utility grid agent is changed from the CON mode to GCCM with $I_G^{ref} = I_{G,pre}^{ref} - \delta_G$. Because the utility grid agent supplies more power to the DC-link before the instant of its DCV sensor fault, $V_{DC,\,i}^{*}$ increases. As $V_{DC,\,i}^{*}$ reaches to $V_{DC,\,W}^{*,L}$, the wind turbine agent can operate in the WDCM to maintain the DCV stabilization. In this case, the battery and EV agents still work in the BCCM and IDLE modes, respectively.

When the third DCV sensor fault occurs in the wind turbine agent, the wind turbine operation is changed to WCCM mode with I_W^{ref} determined as in (15). In this situation, the EV agent changes the operation mode from IDLE mode to EDDM mode to ensure the DCMG system stability, while the utility grid and battery agents keep in GCCM and BCCM. It is confirmed from this simulation test that the proposed scheme still achieves the power balance and voltage regulation if there exists only one DCV sensor which works correctly in the decentralized DCMG.

D. TRANSITION BETWEEN NORMAL AND HIGH ELECTRICITY PRICE CONDITIONS

Fig. 9 shows the simulation results of the proposed scheme for the transition between normal and high electricity price

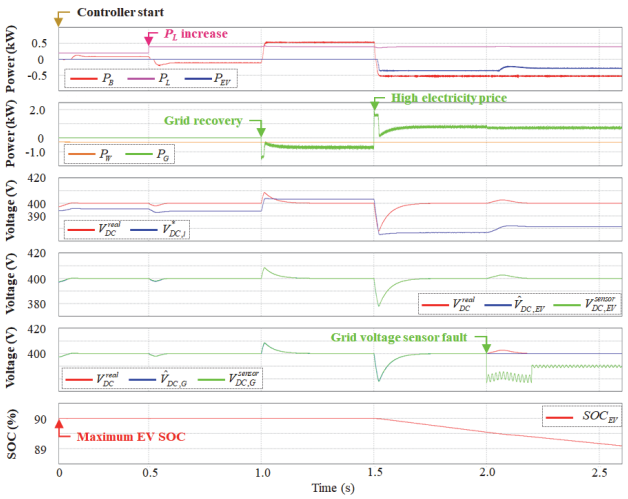

FIGURE 9. Simulation results for the transition between normal and high electricity price conditions under voltage sensor fault.

conditions under voltage sensor fault. The DCMG system starts in the islanded mode, SOC_{EV} is at the highest level, and SOC_B is in the region $[SOC_{min,B}, SOC_{max,B}]$. Because the wind turbine agent supplies power less than the sum of the battery maximum charging power and load demand, the battery agent operates in BDCM mode to maintain the DCV at V_{DC}^{nom}. In this case, the wind turbine and EV agents work in the MPPT and IDLE modes, respectively. As the load power increases at $t = 0.5$ s, the operation mode of the battery agent is changed from BDCM to BDDM to supply the power to the DC-link.

When the utility grid agent is recovered from the fault with the normal electricity price condition at $t = 1.0$ s, the utility grid agent operates in the CON mode with the droop curve D_G to supply power to the DC-link. In this situation, the battery agent switches the operation mode from BDDM to BDCM to absorb maximum power, while the EV and wind turbine agents continue working in IDLE and MPPT modes, respectively.

At $t = 1.5$ s, as the utility grid condition is changed to the high electricity price condition, the $V^* - P$ droop curve of the utility grid is automatically changed from D_G to D_G^{HP} to minimize the utility costs. In this situation, the utility grid agent switches the operation from CON mode to INV mode to absorb the power as much as possible from the DC-link. The battery and EV agents supply the maximum power to the DC-link through BDDM and EDDM, respectively, while the wind turbine operation is still in MPPT mode.

Once the utility grid voltage sensor becomes faulty under the high electricity price condition at $t = 2.0$ s, the operation mode of the utility grid agent is switched from the INV mode to GCCM with $I_G^{ref} = I_{G,pre}^{ref} - \delta_G$. Because the utility grid agent absorbs less power from the DC link before the instant of the DCV sensor fault, $V_{DC,\,i}^*$ increases. As $V_{DC,\,i}^*$ reaches to $V_{DC,\,EV}^{*,L}$, the EV agent can take a control of the DCV

FIGURE 10. Configuration of experimental DCMG test setup.

to ensure voltage stabilization via EDDM. The battery and wind turbine agents keep in the BDDM and MPPT modes to continue injecting the maximum power.

V. EXPERIMENTAL VALIDATIONS

An experimental decentralized DCMG setup as shown in Fig. 10 is utilized to verify the feasibility and reliability of the proposed control scheme. The experimental DCMG system is composed of five power agents: a wind turbine agent, a load agent, a battery agent, an EV agent, and a utility grid agent. The bidirectional DC power sources are utilized as the battery and EV to connect them to the DC-link through the bidirectional interleaved DC/DC converters. The utility grid agent is realized by a three-phase main grid, a transformer, and a bidirectional AC/DC converter with an LCL filter. The wind turbine agent is composed of an AC motor control panel and an induction motor mechanically coupled to a PMSG via a unidirectional AC/DC converter. A digital signal processor (DSP) TMS320F28335 is utilized in each power agent to implement the proposed power management scheme for a decentralized DCMG. Experimental results are presented in several uncertain conditions, including the voltage sensor fault, high electricity price condition, agent power variation, utility grid disconnection, and the different SOC levels of the battery and EV agents with the system parameters listed in Table 2.

A. TRANSITION BETWEEN GRID-CONNECTED MODE AND ISLANDED MODE

Fig. 11 shows the experimental results during the transition from the grid-connected to islanded mode operation. Initially, the decentralized DCMG system is in the grid-connected mode with the normal electricity price condition and SOC_{EV} is at the highest level. Because the generated power of the wind turbine agent is less than the sum of P_L and $P_B^{C,max}$, the utility grid agent regulates the DCV to V_{DC}^{nom} via CON mode according to the droop curve D_G. In this case, the wind turbine, battery, and EV agents operate in MPPT, BDCM, and IDLE modes, respectively.

When the utility grid fault occurs, the DCV value immediately drops because of the power deficit. To ensure the DCV

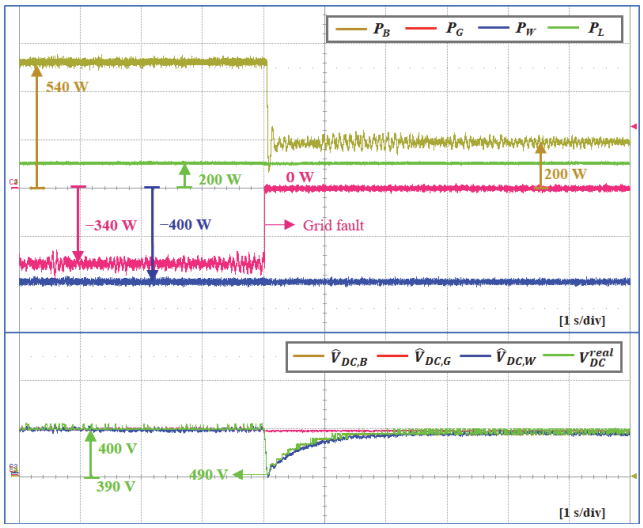

FIGURE 11. Experimental results for the transition from grid-connected mode to islanded mode operation.

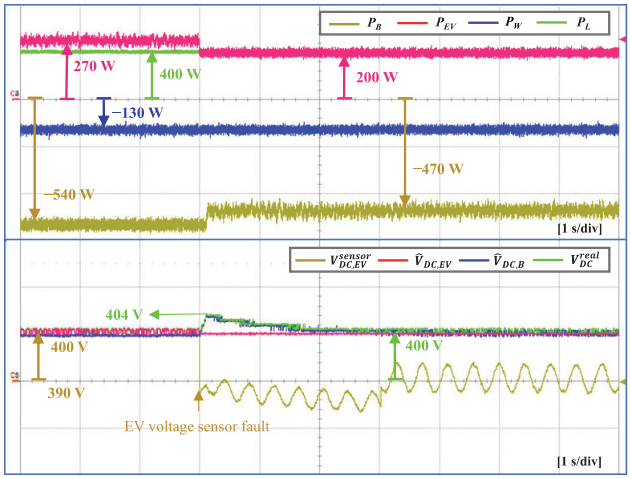

FIGURE 12. Experimental results for the islanded mode under DCV sensor fault in EV agent.

stabilization, the battery agent reduces the charging power via BDCM mode while the wind turbine agent keeps in the MPPT mode.

B. ISLANDED MODE UNDER DCV SENSOR FAULT IN EV AGENT

To verify a seamless power management of the proposed scheme, Fig. 12 shows the experimental results for the islanded mode under the DCV sensor fault in the EV agent. In this test, the decentralized DCMG system initially operates in the islanded mode. Both SOC_B and SOC_{EV} are in the region between the minimum and maximum SOC levels. Because the sum of the power generated by the wind turbine and battery maximum discharging is less than the sum of P_L and $P_{EV}^{C,max}$, the EV agent regulates the DCV to V_{DC}^{nom} while the wind turbine and battery agents operate in MPPT and BDDM modes, respectively. During this time, $\hat{V}_{DC,B}$ and $\hat{V}_{DC,EV}$ accurately track the DCV sensor value $V_{DC,i}$.

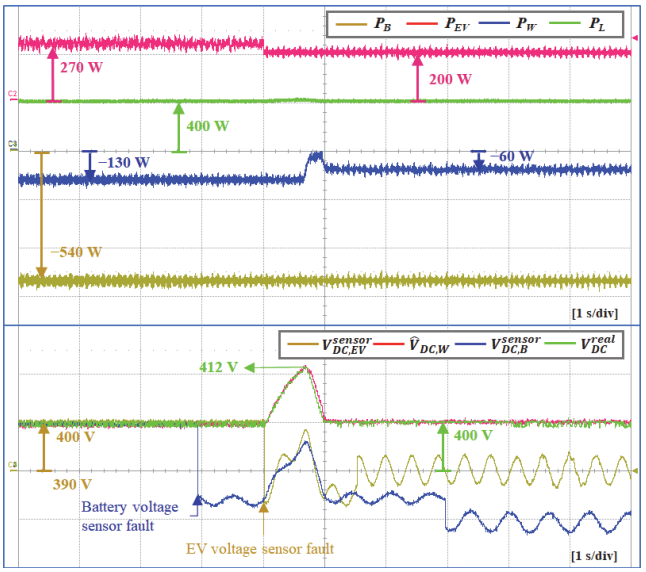

FIGURE 13. Experimental results for the islanded mode under DCV sensor faults in battery and EV agents.

When the DCV sensor of the EV agent suddenly has a fault, the EV agent switches the operation mode from EDCM to ECCM with I_{EV}^{ref} given in (16). Because the EV agent absorbs less power from the DC-link, the DCV increases. As a result, the battery agent controls the DCV to the nominal value via BDDM mode for a continuous power management. The wind turbine agent keeps in MPPT mode.

C. ISLANDED MODE UNDER VOLTAGE SENSOR FAULTS IN BATTERY AND EV AGENTS

To demonstrate the voltage stabilization performance under several voltage sensor faults, the experimental results for the islanded mode are presented in Fig. 13 under DCV sensor faults in the battery and EV agents. Initially, the decentralized DCMG system operates in the islanded mode. Both SOC_B and SOC_{EV} are in the region between the minimum and maximum SOC levels. Before the DCV sensor fault, the EV agent regulates the DCV to V_{DC}^{nom} through EDCM while the wind turbine and battery agents operate in MPPT and BDDM, respectively.

When a fault first occurs in the battery DCV sensor, the battery agent changes the operation mode from BDDM to BCCM with $I_B^{ref} = I_{B,pre}^{ref}$ as in (14). In this situation, the wind turbine and battery agents keep in MPPT and EDCM, respectively.

When another DCV sensor fault occurs in the EV agent that is regulating the DCV, the EV agent switches the operation mode from EDCM to ECCM as soon as the EV agent detects this failure via the fault identification algorithm. The EV current reference I_{EV}^{ref} in ECCM is given by (16). Then, the EV agent decreases the absorbing power from the DC-link, which causes the DCV to increase. To ensure the power balance, the wind turbine agent works in WDCM by maintaining the DCV at the nominal value. It is worth mentioning that only

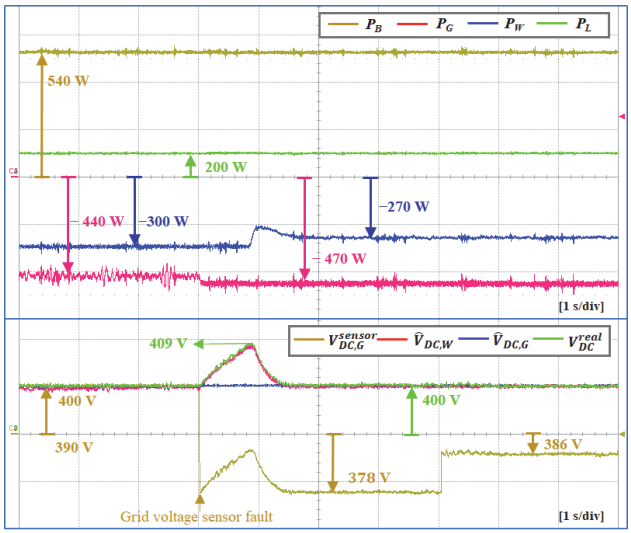

FIGURE 14. Experimental results in the grid-connected mode under DCV sensor fault in utility grid agent.

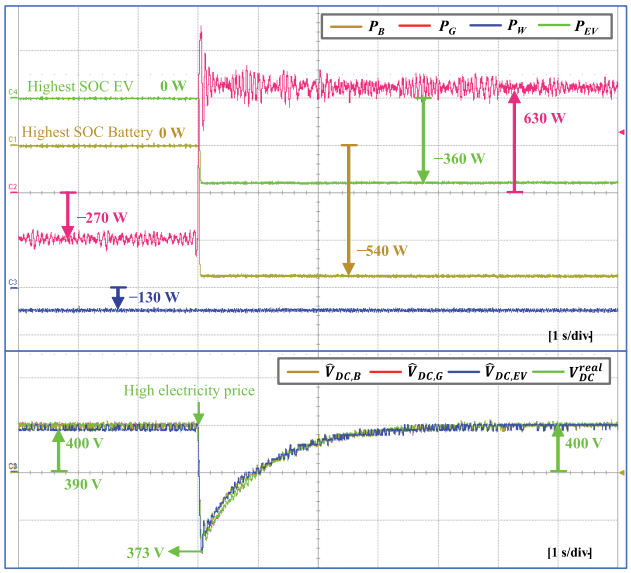

FIGURE 15. Experimental results in the grid-connected mode with electricity price condition change.

the DCV sensor in the wind turbine agents works normally. From this experimental result, it is verified that the proposed scheme can stably and reliably achieve the power balance and voltage regulation even in the presence of several DCV sensor faults.

D. GRID-CONNECTED MODE UNDER DCV SENSOR FAULT IN UTILITY GRID AGENT

Fig. 14 shows the experimental results in the grid-connected mode under the DCV sensor fault in the utility grid agent. Initially, the DCMG system is in the grid-connected mode with the normal electricity price condition and the EV is in the IDLE mode. Because the wind turbine power is less than the load demand, the utility grid agent operates in CON mode to supply the power to the DC-link. In this case, the wind turbine and battery agents operate in MPPT and BDCM, respectively.

When the DCV sensor of the utility grid agent becomes faulty, the utility grid agent changes the operation mode from CON mode to GCCM with $I_G^{ref} = I_{G,pre}^{ref} - \delta_G$ to continue injecting power to the DC-link. As a result, the DCV value increases. Then, the voltage stabilization is achieved by the wind turbine agent by controlling the DCV via WDCM. The battery agent keeps in BDCM mode.

E. GRID-CONNECTED MODE WITH ELECTRICITY PRICE CONDITION CHANGE

To verify the optimal power management of the proposed scheme, Fig. 15 shows the experimental results in the grid-connected mode with the electricity price condition change. The decentralized DCMG system initially operates in the grid-connected mode with the normal electricity price condition, and SOC_B and SOC_{EV} are at the highest level. In this test, the utility grid agent regulates the DCV to V_{DC}^{nom} through CON mode while the wind turbine agent operates in MPPT mode.

When the utility grid condition is changed to the high electricity price condition, the $V^* - P$ droop curve of the utility grid agent is automatically changed from D_G to D_G^{HP} to minimize the utility costs as shown in Fig. 3. In this situation, the utility grid agent changes the operation mode from CON to INV mode to absorb power from the DC-link as much as possible. The wind turbine keeps in MPPT mode, while the battery and EV agents supply the maximum power to the DC-link by BDDM and EDDM modes, respectively.

VI. CONCLUSION

This paper has presented a seamless power management for a decentralized DC microgrid to enhance the voltage and power stabilization under voltage sensor faults. A voltage observer is deployed for each power agent to monitor the voltage sensor abnormality under uncertain conditions such as the agent power variation, battery and EV SOC levels, utility grid disconnection, and high electricity prices. During the normal operations, the proposed control scheme uses the voltage droop control method based on the estimated DCV value to achieve voltage stabilization and power balance. In addition, the droop curve of the utility grid agent is changed automatically to reduce electricity costs under high electricity price condition. To enhance the reliability of the decentralized DCMG under DCV sensor fault, a fault identification algorithm is presented for each power agent to detect voltage sensor failure. Then, a seamless power management has been proposed to ensure the DCMG system stability by switching the voltage droop control mode to the current control mode in which the current magnitude of the power agent with the faulty DCV sensor is changed to perturb the operating point in the droop curves. As a result, the other power agents with the normal DCV sensor can maintain the DCV at the nominal value instead of the power agent with the faulty DCV sensor. Simulation and experimental results under various conditions have demonstrated the effectiveness and reliability of the proposed seamless power management strategy.

REFERENCES

[1] M. H. Saeed, W. Fangzong, B. A. Kalwar, and S. Iqbal, "A review on microgrids' challenges & perspectives," *IEEE Access*, vol. 9, pp. 166502–166517, 2021.
[2] F. Guo, Q. Xu, C. Wen, L. Wang, and P. Wang, "Distributed secondary control for power allocation and voltage restoration in islanded DC microgrids," *IEEE Trans. Sustain. Energy*, vol. 9, no. 4, pp. 1857–1869, Oct. 2018.
[3] E. Espina, J. Llanos, C. Burgos-Mellado, R. Cárdenas-Dobson, M. Martínez-Gómez, and D. Sáez, "Distributed control strategies for microgrids: An overview," *IEEE Access*, vol. 8, pp. 193412–193448, 2020.
[4] D. T. Tran, A. F. Habibullah, and K.-H. Kim, "Seamless power management for a distributed DC microgrid with minimum communication links under transmission time delays," *Sustainability*, vol. 14, no. 22, p. 14739, Nov. 2022.
[5] D.-L. Nguyen and H.-H. Lee, "Enhanced distributed secondary control method for DC microgrids against heterogeneous communication time delays," *J. Power Electron.*, vol. 23, no. 1, pp. 127–138, Jan. 2023.
[6] T. Dragičević, X. Lu, J. C. Vasquez, and J. M. Guerrero, "DC microgrids—Part II: A review of power architectures, applications, and standardization issues," *IEEE Trans. Power Electron.*, vol. 31, no. 5, pp. 3528–3549, May 2016.
[7] M. Kumar, S. C. Srivastava, and S. N. Singh, "Control strategies of a DC microgrid for grid connected and islanded operations," *IEEE Trans. Smart Grid*, vol. 6, no. 4, pp. 1588–1601, Jul. 2015.
[8] T. Van Nguyen and K.-H. Kim, "Power flow control strategy and reliable DC-link voltage restoration for DC microgrid under grid fault conditions," *Sustainability*, vol. 11, no. 14, p. 3781, Jul. 2019.
[9] C. Li, F. de Bosio, F. Chen, S. K. Chaudhary, J. C. Vasquez, and J. M. Guerrero, "Economic dispatch for operating cost minimization under real-time pricing in droop-controlled DC microgrid," *IEEE J. Emerg. Sel. Topics Power Electron.*, vol. 5, no. 1, pp. 587–595, Mar. 2017.
[10] F. A. Padhilah and K.-H. Kim, "A power flow control strategy for hybrid control architecture of DC microgrid under unreliable grid connection considering electricity price constraint," *Sustainability*, vol. 12, no. 18, p. 7628, Sep. 2020.
[11] S. Pannala, N. Patari, A. K. Srivastava, and N. P. Padhy, "Effective control and management scheme for isolated and grid connected DC microgrid," *IEEE Trans. Ind. Appl.*, vol. 56, no. 6, pp. 6767–6780, Nov. 2020.
[12] J. Li, Y. Liu, and L. Wu, "Optimal operation for community-based multi-party microgrid in grid-connected and islanded modes," *IEEE Trans. Smart Grid*, vol. 9, no. 2, pp. 756–765, Mar. 2018.
[13] M. Mehdi, C.-H. Kim, and M. Saad, "Robust centralized control for DC islanded microgrid considering communication network delay," *IEEE Access*, vol. 8, pp. 77765–77778, 2020.
[14] Z. Fan, B. Fan, J. Peng, and W. Liu, "Operation loss minimization targeted distributed optimal control of DC microgrids," *IEEE Syst. J.*, vol. 15, no. 4, pp. 5186–5196, Dec. 2021.
[15] R. Zhang and B. Hredzak, "Distributed finite-time multiagent control for DC microgrids with time delays," *IEEE Trans. Smart Grid*, vol. 10, no. 3, pp. 2692–2701, May 2019.
[16] M. Nabatirad, R. Razzaghi, and B. Bahrani, "Decentralized energy management and voltage regulation in islanded DC microgrids," *IEEE Syst. J.*, vol. 16, no. 4, pp. 5835–5844, Dec. 2022.
[17] X. Li, W. Jiang, J. Wang, P. Wang, and X. Wu, "An autonomous control scheme of global smooth transitions for bidirectional DC–DC converter in DC microgrid," *IEEE Trans. Energy Convers.*, vol. 36, no. 2, pp. 950–960, Jun. 2021.
[18] A. F. Habibullah, F. A. Padhilah, and K.-H. Kim, "Decentralized control of DC microgrid based on droop and voltage controls with electricity price consideration," *Sustainability*, vol. 13, no. 20, p. 11398, Oct. 2021.
[19] F. Guo, C. Deng, C. Wen, X. Zheng, Z. Lian, and W. Jiang, "Partially decentralized secondary current sharing and voltage restoration controller design for DC microgrids with event-triggered sampling," *IEEE Trans. Smart Grid*, vol. 14, no. 3, pp. 1777–1789, May 2023.
[20] Q. Song, L. Wang, and J. Chen, "A decentralized energy management strategy for a fuel cell–battery hybrid electric vehicle based on composite control," *IEEE Trans. Ind. Electron.*, vol. 68, no. 7, pp. 5486–5496, Jul. 2021.
[21] N. Vafamand, M. M. Arefi, M. H. Asemani, M. S. Javadi, F. Wang, and J. P. S. Catalão, "Dual-EKF-based fault-tolerant predictive control of nonlinear DC microgrids with actuator and sensor faults," *IEEE Trans. Ind. Appl.*, vol. 58, no. 4, pp. 5438–5446, Jul. 2022.
[22] A. Vafamand, B. Moshiri, and N. Vafamand, "Fusing unscented Kalman filter to detect and isolate sensor faults in DC microgrids with CPLs," *IEEE Trans. Instrum. Meas.*, vol. 71, pp. 1–8, 2022.
[23] K. Jessen, M. Soltani, and A. Hajizadeh, "Sensor fault detection for line regulating converters supplying constant power loads in DC microgrids," in *Proc. IEEE 11th Int. Symp. Power Electron. Distrib. Gener. Syst. (PEDG)*, Sep. 2020, pp. 99–103.
[24] M. Huang, L. Ding, W. Li, C.-Y. Chen, and Z. Liu, "Distributed observer-based H_∞ fault-tolerant control for DC microgrids with sensor fault," *IEEE Trans. Circuits Syst. I, Reg. Papers*, vol. 68, no. 4, pp. 1659–1670, Apr. 2021.
[25] A. F. Habibullah and K.-H. Kim, "Decentralized power management of DC microgrid based on adaptive droop control with constant voltage regulation," *IEEE Access*, vol. 10, pp. 129490–129504, 2022.

DAT THANH TRAN was born in Hà Tĩnh, Vietnam, in 1995. He received the B.S. degree in control engineering and automation from the Hanoi University of Science and Technology, Hanoi, Vietnam, in 2018. He is currently pursuing the M.S. degree in electrical and information engineering with the Seoul National University of Science and Technology, Seoul, South Korea. His current interests include control theory, power electronics, renewable energy, and microgrids.

MYUNGBOK KIM (Member, IEEE) was born in Daegu, South Korea, in 1973. He received the B.S. degree in electronics engineering from Kyungpook National University, Daegu, in 1996, and the M.S. and Ph.D. degrees in electrical engineering from the Korea Advanced Institute of Science and Technology (KAIST), Daejeon, South Korea, in 1998 and 2010, respectively. From 2005 to 2010, he was a Research and Development Engineer with Fairchild Semiconductor (now ON Semiconductor), South Korea, where he was engaged in the research and development of smart power module. In 2010, he was a Senior Research and Development Engineer with Siliconworks (now LX Semicon), South Korea, where he was engaged in the research and developed of display driver ICs. Since December 2010, he has been with Korea Institute of Industrial Technology, Gwangju, South Korea, where he is currently a Principal Researcher. His current research interests include digital power conversion systems, compound semiconductor applications, and various MCU-controlled applications. He is a member of the Korean Institute of Power Electronics (KIPE).

KYEONG-HWA KIM (Senior Member, IEEE) was born in Seoul, South Korea, in 1969. He received the B.S. degree in electrical engineering from Hanyang University, Seoul, in 1991, and the M.S. and Ph.D. degrees in electrical engineering from the Korea Advanced Institute of Science and Technology (KAIST), Daejeon, South Korea, in 1993 and 1998, respectively. From 1998 to 2000, he was a Research Engineer with Samsung Electronics Company, South Korea, where he was engaged in the research and development of AC machine drive systems. From 2000 to 2002, he was a Research Professor with KAIST. From August 2010 to August 2011, he was a Visiting Scholar with the Virginia Polytechnic Institute and State University (Virginia Tech), Blacksburg, VA, USA. Since August 2002, he has been with the Seoul National University of Science and Technology, Seoul, where he is currently a Professor. His current research interests include AC machine drives, the control and diagnosis of power systems, power electronics, renewable energy, and DSP-based control applications. He is a member of the Korean Institute of Power Electronics (KIPE).